BIOINFORMATICS ORIGINAL PAPER

Vol. 26 no. 5 2010, pages 653–660
doi:10.1093/bioinformatics/btq018

Systems biology

Advance access publication January 22, 2010

Computational quantification of metabolic fluxes from a single isotope snapshot: application to an animal biopsy

Thomas W. Binsl[1], David J.C. Alders[2], Jaap Heringa[1], A.B. Johan Groeneveld[2] and Johannes H.G.M. van Beek[1,2,*]

[1]Centre for Integrative Bioinformatics, VU University Amsterdam, 1081HV Amsterdam and [2]VU University Medical Centre, 1081BT Amsterdam, The Netherlands

Associate Editor: Olga Troyanskaya

ABSTRACT

Motivation: Quantitative determination of metabolic fluxes in single tissue biopsies is difficult. We report a novel analysis approach and software package for *in vivo* flux quantification using stable isotope labeling.

Results: We developed a protocol based on brief, timed infusion of ^{13}C isotope-enriched substrates for the tricarboxylic acid (TCA) cycle followed by quick freezing of tissue biopsies. NMR measurements of tissue extracts were used for flux estimation based on a computational model of carbon transitions between TCA cycle metabolites and related amino acids. To this end, we developed a computational framework in which metabolic systems can be flexibly assembled, simulated and analyzed. Flux parameters were quantified from NMR multiplets by a partial grid search followed by repeated Nelder–Mead optimizations implemented on a computer grid. We implemented a model of the TCA cycle and showed by extensive simulations that the timed infusion protocol reliably quantitates multiple fluxes. Experimental validation of the method was done *in vivo* on hearts of anesthetized pigs under two different conditions: basal state ($n=7$) and cardiac stress caused by infusion of dobutamine ($n=7$). About nine tissue samples (40–200 mg dry-weight) were taken per heart. TCA cycle flux was 6.11 ± 0.28 (SEM) μmol/min·gdw at baseline versus 9.29 ± 1.03 μmol/min·gdw for dobutamine stress. Oxygen consumption calculated from the TCA cycle flux and from 'gold standard' blood gas-based measurements were close, correlating with $r=0.88$ ($P<10^{-4}$). Spatial heterogeneity in metabolic fluxes is detectable amongst the small samples. We propose that our novel isotope snapshot methodology is suitable for flux measurements in biopsies *in vivo*.

Availability: Non-profit organizations will, upon request, be granted a non-exclusive license to use the software for internal research and teaching purposes at no charge. A web interface for using the software on our computer grid is available under http://www.ibi.vu.nl/programs/

Contact: hans.van.beek@falw.vu.nl

Supplementary information: Supplementary data are available at *Bioinformatics* online.

Received on August 25, 2009; revised on November 27, 2009; accepted on January 8, 2010

*To whom correspondence should be addressed.

1 INTRODUCTION

Metabolic fluxes reflect the function and dynamics of cells in the body. However, measuring metabolic fluxes in small tissue samples in animals *in vivo* is very difficult and needs (i) a special experimental strategy and (ii) sophisticated computational analysis. Measurement of metabolic fluxes in whole organs or large tissue volumes was possible by measuring time series of ^{13}C incorporation in intermediary metabolites with *in vivo* NMR spectroscopy (Chance *et al.*, 1983; Malloy *et al.*, 1990). van Beek *et al.* (1998, 1999) developed a strategy to infuse substrates enriched with stable isotopes for several minutes and arrest metabolism before a steady state of label incorporation is attained. Metabolic fluxes are then quantitated by computational analysis from NMR measurements on a single tissue sample collected at a single time point. Given the usually quite heterogeneous metabolism of tissue, this approach overcomes the difficulty that a time series of metabolite levels cannot be obtained from one small biopsy in tissue. However, an advanced computational analysis is key to successfully perform these metabolic flux measurements *in vivo* and is presented here.

It was desirable to optimize the original computational analysis strategy and software to quantitate fluxes from biopsies. This analysis was originally built on a package optimized for indicator-dilution studies in a PET setting (van Beek *et al.*, 1999). The underlying models were built on early pre-steady-state labeling work (Chance *et al.*, 1983; Malloy *et al.*, 1990; van Beek *et al.*, 1998, 1999). Meanwhile, further non-steady-state approaches have been developed with applications in biotechnology (Nöh and Wiechert, 2006). Here, we present a new analysis approach optimized for the single time point analysis applicable to biopsies. This approach is embedded in a software package that makes it possible to build carbon transition models for arbitrary metabolic pathways without the need to apply a computer programming language.

Metabolic fluxes can be measured by infusion of substrates labeled with radioactive or stable isotopes. Usually the time course of incorporation of label is followed, for instance, by *in vivo* NMR spectroscopy, or label is infused sufficiently long that a stable steady state is reached. In the latter case relative fluxes can be determined, and if uptake from outside the cells can be measured, absolute fluxes can be derived. Under *in vitro* conditions, uptake of a substrate can often easily be measured. For instance, the decrease of glucose in cell culture medium gives its uptake in the cells. However, it is difficult to measure uptake of substrate in small regions in the body from the blood. This would require measurement of metabolite

levels in the venous blood, which is feasible for whole organs but difficult for small regions due to the small size and dense interconnection of venules and veins. On the other hand, the spatial and biochemical resolution of non-invasive spectroscopic imaging techniques is insufficient.

Most existing methods and software [e.g. OpenFLUX (Quek *et al.*, 2009)] developed for flux estimation require the close approximation of a steady state of isotope label incorporation (Antoniewicz *et al.*, 2007; Kelleher, 2001; Sherry *et al.*, 2004; Wiechert, 2001). This leads to long experiments requiring a large amount of isotope-enriched substrate and is particularly challenging in mammalian experiments, where metabolic steady states are often brief. To solve these problems, methods for quick flux quantification have been designed (van Beek *et al.*, 1998, 1999). In contrast with previously developed methods, metabolism is arrested before an isotopic steady state is reached and samples are taken. This generates a snapshot of labeling at one time point. The extent of isotope incorporation in carefully chosen key metabolites in the sample is measured. Hence, using this experimental strategy, which we term Labeling with Isotope for Pre-Steady-State Snapshots (LIPSSS), only a single time point measurement is needed to quantify multiple metabolic fluxes.

The LIPSSS method was previously validated in isolated hearts (van Beek *et al.*, 1998, 1999). However, an enhanced computational analysis able to analyze LIPSSS data including a validation of this new flux analysis approach *in vivo* is highly desirable. To this end, a flexible and improved simulation and analysis algorithm is implemented in a software package named FluxEs, described here. The software package allows assembling the model equations for arbitrary metabolic systems using a simple input format. This avoids extensive computer programming to hard code the metabolic pathways and experimental protocols. Hence, FluxEs facilitates a flexible application to a broad range of metabolic systems and enables life scientists without computer programming skills to simulate and analyze stable isotope experiments.

Parameter estimation in large metabolic systems is a great challenge, particularly because a certain fraction of the model parameters typically shows low sensitivity and 'sloppiness' (Gutenkunst *et al.*, 2007). The latter term means among others that the predicted results are insensitive to certain parameter combinations, but very sensitive to correlated changes in other parameter combinations. In particular, parameters in these models often exhibit least squares cost landscapes, which show 'golf course' characteristics with shallow slopes and multiple narrow minima (Brown and Sethna, 2003). Hence, we describe a new parameter optimization strategy suitable to handle such metabolic systems, implemented in FluxEs. The strategy that additionally includes suitable error estimation of the quantified fluxes and possible incorporation of prior knowledge via Bayesian priors was developed by extensive computer simulations.

To validate the new analysis approach, we analyzed LIPSSS data obtained from experiments on mammalian hearts *in vivo* under two metabolic conditions: seven hearts studied under baseline conditions, which had been analyzed before with the old algorithms (Alders *et al.*, 2004) and seven new hearts studied under dobutamine stress to increase metabolism. To experimentally validate the new analysis algorithms for the LIPSSS method in FluxEs, the results were compared with a 'gold standard' method to quantify aerobic metabolism in whole hearts using blood oxygen measurements.

The FluxEs package runs in the R environment which is open source. R is available on different computing platforms (MS Windows, Linux, Macintosh, etc.), and is widely used for statistical data analysis, for instance of microarray gene expression data.

In summary, we describe a new method for flux quantification based on LIPSSS experiments. We present a computer package (FluxEs) to easily implement computer models for arbitrary metabolic pathways and quantify fluxes by estimating model parameters. Compared with our earlier pre-steady-state analysis approach (Alders *et al.*, 2004; van Beek *et al.*, 1998, 1999), the method described in this article includes a tailored approach to parameter optimization necessary for flux estimation, including error analysis and use of prior knowledge. It was developed and its properties were assessed based on a large number of computer simulations. Finally, we validate the overall approach experimentally on tissue samples taken during *in vivo* experiments on porcine hearts.

2 METHODS

2.1 LIPSSS method and tricarboxylic acid cycle model

The investigation of biological systems using LIPSSS experiments involves a timed, brief infusion of a substrate enriched with isotopic labels into the metabolic system (van Beek *et al.*, 1998, 1999). For instance, ^{13}C may be enriched in glucose or acetate, replacing the highly natural abundant ^{12}C. Metabolism in the sample is stopped at a predefined time before an isotopic steady state is reached. The isotope labels are distributed by biochemical reactions and cause different combinations of isotopes, termed isotopomers, in particular metabolite pools. For instance, two carbon metabolites such as acetate or acetyl coenzyme A may consist of four isotopomers: $^{12}C^{12}C$, $^{12}C^{13}C$, $^{13}C^{12}C$ and $^{13}C^{13}C$.

Depending on the metabolic fluxes all metabolite pools have a characteristic composition of isotopomer fractions at each time point of the dynamic phase before reaching isotopic steady state. Consequently, fluxes can be determined from measurements reflecting isotopomer fractions (van Beek *et al.*, 1998, 1999). Unfortunately, only relative flux contributions can be quantified if an isotopic steady state has been reached. However, before isotopic equilibrium the isotope enrichment measurements yields sufficient information to quantify absolute flux values. Single isotopomer fractions or cumulated contributions of several different isotopomers are reflected by distinct line intensities in single time point measurements done with NMR spectroscopy or mass spectrometry (MS). The line intensities predicted by model analysis depend on the metabolic fluxes, and reversely, measured line intensities allow quantifying fluxes in the biological system (Section 2.3). The model applied in this study (Fig. 1) was modified from a model of the TCA cycle described previously (van Beek *et al.*, 1998, 1999). Although any metabolic pathway is easily implemented using the new computer package (Supplementary Material), this TCA cycle model was chosen to demonstrate the computer package because it applies to the validation experiments (see below). The model consists of 10 metabolite pools: eight pools with a finite metabolite content and two implemented as 'virtual' pools with negligible amounts of metabolites. Such virtual pools were previously introduced in mathematical models for isolated heart NMR experiments by Malloy *et al.* (1990). They are implemented with algebraic equations rather than differential equations and mix converging metabolic fluxes without any time delay. This approximates mixing of several metabolic fluxes in small metabolite pools exhibiting fast turnover rates.

Carbon is transferred between metabolites, from one specific atomic position in one pool to another specific position in the next pool. In the TCA cycle model, 50 such carbon transitions link the metabolites. The model has been validated with *in vivo* NMR spectroscopy time course data (van Beek *et al.*, 1999).

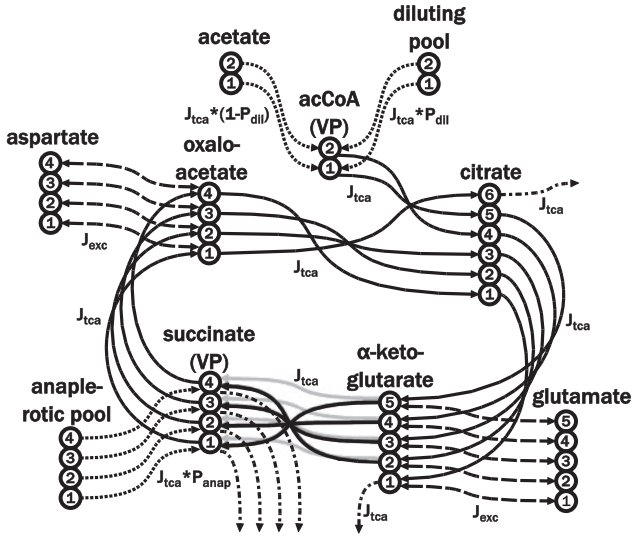

Fig. 1. The carbon transition network of the TCA cycle consists of 10 metabolic pools: (1) acetate, (2) diluting pool that accounts for admixture of other substrates forming acetyl coenzyme A (acCoA) such as carbohydrates and fatty acids, (3) acCoA, (4) citrate (also representing *cis*-aconitate and isocitrate), (5) α-ketoglutarate, (6) glutamate, (7) anaplerotic pool, (8) succinate, (9) oxaloacetate (also representing fumarate and malate) and (10) aspartate. acCoA and succinate are implemented as 'virtual' pools (VP, see text). Each circle represents a carbon atom and each string of circles a molecule. The numbers in the circles give the numbering of the carbon atoms according to standard nomenclature. Fluxes entering the system are presented as dotted arrows, while fluxes leaving the system are illustrated as dashed-dotted arrows. The two exchange fluxes between TCA cycle intermediates and amino acids are indicated by dashed arrows. TCA cycle flux is given by continuous arrows. Half of the flux between α-ketoglutarate and succinate is going via one branch (black arrows), the other half is going via the other branch (gray arrows), reversing the carbon chain in the symmetric metabolite. For parameter descriptions see text.

The model contains five parameters. J_{tca} (μmol/min·gdw) is the absolute TCA cycle flux and considered to be constant over the entire TCA cycle. J_{exc} (μmol/min·gdw) is an exchange flux swapping (i) α-ketoglutarate carbon skeleton with glutamate and (ii) aspartate's skeleton with oxaloacetate back and forth by transamination. The fractional parameter P_{dil} accounts for the relative dilution of the flux from labeled acetate into the acetyl coenzyme A pool by unlabeled substrates such as glucose, glycogen, fatty acids, etc., and reflects relative carbon substrate fluxes. The fractional anaplerotic flux P_{anap} accounts for the relative anaplerotic dilution of the TCA cycle flux with metabolites, which remain unlabeled at early time points, during infusion of enriched substrate (Sherry *et al.*, 2004). Since pyruvate carboxylase activity, which underlies anaplerosis into the oxaloacetate pool, is less important in heart tissue, we did not incorporate additional anaplerotic flux into the oxaloacetate pool (Pound *et al.*, 2009). Finally, the time constant T_{trans} (min) describes the exponential accumulation of ^{13}C label in acetyl coenzyme A from infused ^{13}C-acetate (Randle *et al.*, 1970; van Beek *et al.*, 1999). The myocardial oxygen consumption M_{VO_2} (μmol/min·gdw) linked to oxidative phosphorylation is calculated from two of the parameters (Chatham *et al.*, 1995):

$$M_{VO_2} = (2 + P_{dil}) J_{tca} \quad (1)$$

2.2 Experimental data

LIPSSS experiments were done on two groups of pigs studied under anesthesia: basal state [$n = 7$, control group, previously analyzed with the old algorithms in Alders *et al.* (2004)] and cardiac stress caused by dobutamine infusion ($n = 7$, dobutamine group). Additionally, for each heart oxygen consumption was calculated from blood gas and blood flow measurements. All experiments were performed according to the following protocol: after the pigs were anesthetized, a continuous infusion of unlabeled acetate into the left descending coronary artery was initiated to establish a metabolic baseline within 6 min (Randle *et al.*, 1970). Dobutamine (10–15μg/min·kg) was given via peripheral venous infusion in the second group. After 30 min the infusion of unlabeled acetate was instantly replaced by an equally concentrated [2-^{13}C] acetate infusion for 4 min. Finally, a second switch was made to [1,2-^{13}C] acetate for an additional 90 s. For a detailed description we refer to Alders *et al.* (2004)

The oxygen content of venous blood coming from the whole left ventricle was measured in blood samples from the coronary sinus with a blood gas analyzer. Local blood flow was measured using radioactively labeled microspheres in the same tissue regions as used for ^{13}C NMR spectroscopy. The blood gas and blood flow measurements were then used to calculate the oxygen consumption within the heart. An $\sim$4 cm^2 large area of the anterior left ventricular free wall of the cardiac tissue was excised, flash-frozen, freeze-dried and subdivided into smaller parts. The subdivision led to about nine tissue biopsies for each heart (40–200 mg dry weight). Finally, metabolites were extracted from these biopsies using perchloric acid and glutamate's ^{13}C NMR multiplets measured (Alders *et al.*, 2004). Up to nine independent multiplets were obtained and analyzed by the FluxEs program to estimate the parameters of the TCA cycle model (Section 2.3).

2.3 Computer package and flux parameter optimization

Knowledge of metabolic flux parameters is crucial to understand metabolism. Therefore, we developed a computer package, named FluxEs, which applies new analysis algorithms (see below) for the estimation of metabolic parameters using information of isotopomer distributions. FluxEs is based on our previously developed program FluxSimulator (Binsl *et al.*, 2007), which allowed simulation of isotopomer distributions but did not include parameter estimation. FluxEs is running in the R computational environment and is compatible with all operating systems on which R is implemented. Hence, it was easy to port FluxEs from a desktop to the Dutch Life Science Grid where all computations were performed. FluxEs accepts an easy input format that offers non-computer scientists a convenient and flexible way to specify arbitrary metabolic models in a plain text file (Supplementary Material). Using the information about the metabolic pathway and its carbon transitions, the ordinary differential equations (ODEs) representing the mathematical model are automatically assembled and the user is guided through the optimization setup via command-line inputs. A description of the systems of differential equations representing such models is given in Binsl *et al.* (2007) and for the TCA cycle model example in van Beek *et al.* (1999).

By solving the ODEs via numerical integration [ODE solver by Hindmarsh (1983)], isotopomer fractions evolving over time are calculated for each metabolite pool of the model. The pool concentrations were taken from Alders *et al.* (2004) and van Beek *et al.* (1999). During parameter estimation the integration routine continuously calculates these isotopomer fractions using different parameter estimates provided by the optimization algorithm. An example of dynamically evolving isotopomer fractions is given in Figure S1 (Supplementary Material). The isotopomer fractions, determined for the time point at which the sample is taken in the experiment, are then used to calculate simulated ^{13}C NMR multiplet intensities m_{sim}. These simulated NMR multiplet intensities are compared with the experimental NMR multiplets m_{exp} (van Beek *et al.*, 1999) and weighted by the standard deviation (SD) σ of the multiplet measurement value for that time point (χ^2 scoring function). The SDs of the intensities are derived from the NMR-free induction decay signal by the analysis package AMARES (Vanhamme *et al.*, 1997). A Bayesian prior with previous knowledge about a parameter can be added to the cost function. In this term $\hat{p}$ is the expected value of the parameter, p the current value of the parameter

and $\sigma^{\log}$ the standard error of the logarithm (base e) of the parameter based on prior knowledge. The parameters giving the minimum χ^2_{prior} by a nonlinear least square procedure are reported.

$$\chi^2_{\text{prior}} = \sum_{i \in \text{multiplets}} \left(\frac{m^i_{\text{sim}} - m^i_{\text{exp}}}{\sigma_i} \right)^2 + \sum_{j \in \text{priors}} \left(\frac{\log(\hat{p}_j) - \log(p_j)}{\sigma^{\log}_j} \right)^2 \quad (2)$$

2.4 Parameter exploration and simulation

Initially, the flux estimation procedure was extensively tested on synthetic noisy data to find an optimal strategy to estimate the parameters of the TCA cycle model. Eight relevant metabolic states to be simulated were defined based on the experimental data: the samples of the control group ($n = 63$) and the dobutamine group ($n = 56$) were hierarchically clustered (complete linkage) according to their NMR multiplet intensities. We discovered four clusters in the control (CL^1_{con}, CL^2_{con}, CL^3_{con}, CL^4_{con}) and four clusters in the dobutamine group (CL^1_{dob}, CL^2_{dob}, CL^3_{dob}, CL^4_{dob}). Clusters within and among the groups differed in the number of detectable multiplets and multiplet intensities. To generate eight synthetic datasets corresponding to the clusters the following steps were performed.

The sample closest to the average of the cluster's samples was chosen as representative. Then the experimental protocol introduced in Section 2.2 was simulated with parameter values for J_{tca}, J_{exc}, T_{trans}, P_{dil} and P_{anap} giving synthetic NMR multiplets close to the representative sample. According to prior knowledge found in the literature (Martini *et al.*, 2002; Panchal *et al.*, 2000, 2001), the relative anaplerosis of the TCA cycle flux P_{anap} was set to 6% of the TCA cycle flux during the simulations.

In order to put realistic noise on the synthetic multiplets, we averaged the standard errors of the NMR measurements for each multiplet in the cluster. This error was added as Gaussian noise to the particular simulated multiplet. For instance, the average relative standard error of all singlets of the third carbon atom of glutamate (*S3*) in cluster CL^1_{con} was 11.1%. Hence, 11.1% Gaussian noise was added to the simulated *S3* value. Finally, for all multiplets it was checked whether intensities had become lower with the added noise than the minimum intensity measurable for that multiplet in the cluster. Such multiplets were considered not detectable and removed from the simulated data. Following this procedure 25 noisy datasets were generated for each cluster.

χ^2_{prior} cost surfaces were visualized using 2D contour plots with pairs of parameters as variables while keeping the remaining parameters fixed. The composition of the surface is defined by the χ^2_{prior} between multiplets simulated with reference parameter values and multiplets computed for parameter values deviating from the reference. Example contour plots are shown in Figure 2 and discussed in Section 3. Using the contour plots the parameter space was explored to discover (i) parameter sensitivities to variations of other parameters and (ii) parameter combinations that give little variation in model prediction. The latter are termed 'sloppy' directions in parameter space (Gutenkunst *et al.*, 2007).

2.5 Parameter optimization

The simulation studies demonstrated that parameter estimation in shallow parameter landscapes using random start values is a challenge. To improve this situation, a new strategy was developed to guide the optimization to the global optimum. First, the parameter space of dimension $n = 5$ parameters was covered by a grid. The grid points were all combinations of: $J_{\text{tca}} = (1, 2, 4, 8, 16, 32, 64)$ µmol/min·gdw, $J_{\text{exc}} = (1, 2, 4, 8, 16, 32, 64)$ µmol/min·gdw, $T_{\text{trans}} = (0.1, 0.3, 0.5, 0.7, 0.9)$ min, $P_{\text{anap}} = (0.1, 0.3, 0.5, 0.7, 0.9)$ and $P_{\text{dil}} = (0.1, 0.3, 0.5, 0.7, 0.9)$. Afterwards, for every grid point its χ^2_{prior} value was calculated and the 10 grid points with the lowest χ^2_{prior} value were used as starting points for the subsequent parameter estimation. To avoid missing those regions which are on average low but without a particularly low grid point on a corner, the parameter space was covered with n-dimensional polyhedrons using the grid points as vertex points. To quantitate the average level of a polyhedron's part of the parameter space, the average χ^2_{prior} value of all vertices belonging to that polyhedron was determined. For each of the 10 polyhedrons with the lowest average χ^2_{prior} value, its vertex with lowest χ^2_{prior} and the polyhedrons center point (arithmetic mean) was determined. These two values were additionally used as starting points for the parameter estimation. Grid points selected multiple times were only used once. To choose reasonable exploration ranges, prior knowledge from literature on maximal enzyme capacities and maximal measured fluxes is used to cover the complete feasible region.

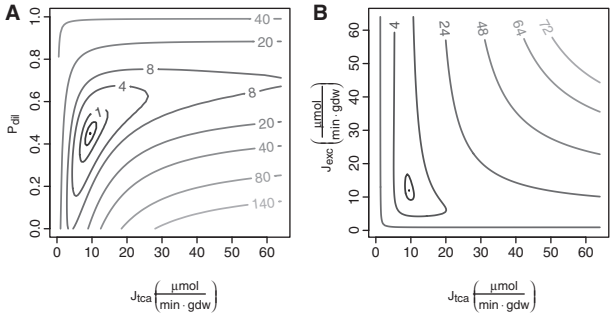

Fig. 2. Two contour plots of χ^2_{prior} in the plane defined by different model parameter combinations, plotted around the region of the global minimum. Parameters J_{tca} and P_{dil} show a more diagonal and elliptic shape of the χ^2_{prior} landscape around the global optimum at point $J_{\text{tca}} = 9.5$ µmol/min·gdw and $P_{\text{dil}} = 0.45$ (**A**). Insensitivity of parameter J_{exc} is shown by vertical elliptic χ^2_{prior} landscape around the global optimum located at $J_{\text{tca}} = 9.5$ µmol/min·gdw and $J_{\text{exc}} = 12$ µmol/min·gdw (**B**). The synthetic data are noise free. Corresponding plots using Gaussian noise as described in Section 2 are given in Supplementary Figure S2.

After generating the synthetic datasets with known parameter values and finding good start positions (see previous paragraph), a fitting procedure was used to re-estimate the 'true' parameters for all clusters. The parameter fitting was done by a downhill simplex optimization (Nelder–Mead) with three consecutive stages. Each stage was terminated when either the relative change in χ^2_{prior} was below 10^{-8} or a maximum number of 500 iterations was achieved. While the first stage used the initial start values for optimization, the two subsequent stages utilize the parameter estimates achieved by the preceding optimization module to continue the optimization. This multiple stage strategy enables optimization algorithms to escape local minima. The Nelder–Mead optimization was chosen due to better performance in re-estimating known parameter values of the TCA cycle model compared with other approaches (see Supplementary Material for a comparison of different optimization routines). All parameters were constrained according to literature information (Carvalho *et al.*, 2001; Sherry *et al.*, 1998) in the following intervals: $J_{\text{tca}} = [0, 64]$ µmol/min·gdw, $J_{\text{exc}} = [0, 64]$ µmol/min·gdw, $T_{\text{trans}} = [0, 5]$ min, $P_{\text{dil}} = [0, 1]$ and $P_{\text{anap}} = [0, 1]$. Additionally, the parameter P_{anap} was coupled to a Bayesian prior with an expected value of $6\% \pm 3\%$ of the TCA cycle flux.

The results of the parameter re-estimation are discussed in Section 3 and given in Figure 3. They show that the estimations of the TCA cycle flux J_{tca}, the transition time T_{trans} and the relative dilution of the labeled acetyl coenzyme A pool P_{dil} work well. As expected the parameter estimation of P_{anap} works properly due to the Bayesian prior. However, the estimation of the exchange flux J_{exc} shows bias and has a larger SD especially in the clusters characterized by few detectable multiplet peaks. In order to improve the estimation of the parameters J_{tca} and P_{dil}, we constrained the parameters J_{exc} and T_{trans} with additional Bayesian priors derived from the measured samples with many detectable multiplets (see below).

Error calculations for each individual sample are possible using the asymptotic standard error for the linearized model [Equation (3)], although not a priori guaranteed to give accurate results. For the linearized calculation Bayesian constrained parameters were kept fixed. Simulations showed that

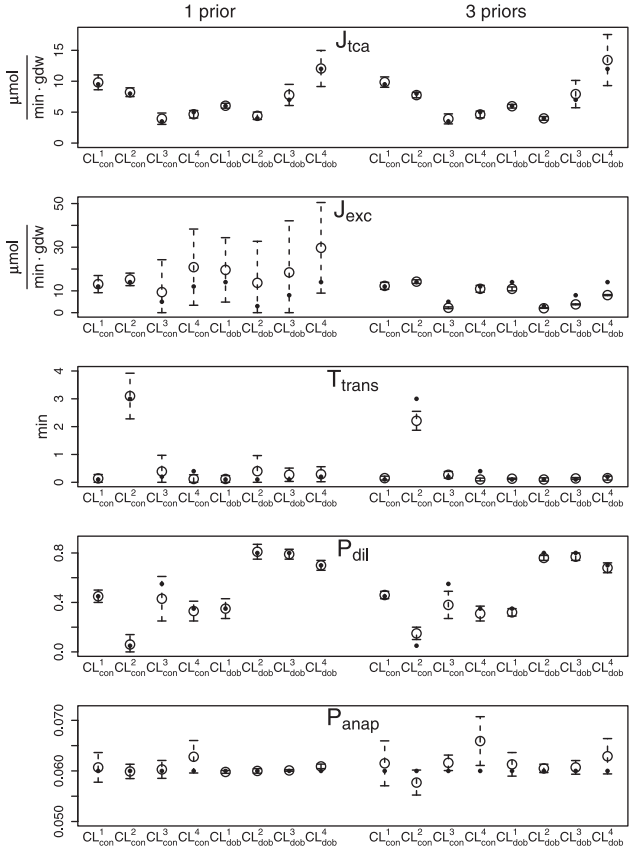

Fig. 3. Average parameter estimates (open circles) with standard error (bars) achieved on the eight clusters using (i) the model with a Bayesian prior on P_{anap} only (left) and the model using Bayesian priors on P_{anap}, J_{exc} and P_{dil} (right). The 'true' parameter values are given as black dots.

the linearized approach gives similar standard errors as the variation shown by 25 simulations of the non-linear model with noise (Supplementary Table S1). Equation (3) gives the square root of the variance–covariance matrix of parameter estimates as function of the Jacobian J (NMR multiplets across rows and parameters across columns) and the inverse of the diagonal matrix of the multiplet's standard errors Δ^{-1}. Superscript T indicates the transpose.

$$E = \sqrt{(J^{\mathrm{T}}\Delta^{-1}J)^{-1}} \tag{3}$$

Asymptotic error calculations [Equation (3)] on the simulations often predicted high errors for J_{exc} and T_{trans}, especially on datasets with a low number of detectable multiplets. Hence, we constrained these two parameters with additional Bayesian priors derived from those datasets that gave low error in the parameter estimates. In these datasets we included all estimates with linearized error estimates up to twice the minimum error found amongst the simulations. These minimum error estimates were 2.87 µmol/min·gdw (cluster CL^2_{con}) for the minimum SD of J_{exc} and 0.13 min for T_{trans} (cluster CL^1_{con}), respectively. From the accepted values the average and SD were determined per cluster and combined into a Bayesian prior for J_{exc} and T_{trans}. These priors were than used in addition to the prior for P_{anap}. This additional prior knowledge improves the estimation of the two parameters (J_{tca} and P_{dil}) that are in particular important for measuring energy metabolism. Please note that the estimated values of the parameters constrained by Bayesian priors have of course little value for the individual samples. The results of the parameter estimation using the three priors are given in Figure 3 and show that the standard error of the estimate of J_{tca} and P_{dil} was decreased by 19% and 39% on average relative to one prior.

The parameter fitting procedure with three priors was applied to the measured samples. Finally, all samples with errors on J_{tca} and P_{dil} higher than twice the maximum values found in simulations of the control group (0.205 µmol/min·gdw for J_{tca} in cluster CL^3_{con} and 0.329 for P_{dil} in cluster CL^2_{con}) were rejected for further analysis.

The oxygen consumption for each heart $MV_{O_2}^{heart}$ (µmol/min·gdw) was computed by adding its individual biopsy oxygen consumptions $MV_{O_2}^{biopsy}$ (µmol/min·gdw) [Equation (1)] weighted by their dry weights, w^{biopsy} (g dry mass), and divided by the sum of all dry weights [Equation (4)]. At least two samples per heart had to pass the quality criterion. The calculated oxygen consumptions were then compared with the 'gold standard' blood gas oxygen consumptions measured in the experiments.

$$MV_{O_2}^{heart} = \frac{\sum_{biopsies} w^{biopsy} MV_{O_2}^{biopsy}}{\sum_{biopsies} w^{biopsy}} \tag{4}$$

This comparison is valid since despite intensive research (Bassingthwaighte and Beard, 1995; Prinzen and Bassingthwaighte, 2000) designated anatomical regions with consistently higher enzyme activities or blood flow have not been found. Hence, oxygen consumption in several small regions can be added and compared with measured oxygen consumption for the total region which encompasses the small regions plus surrounding regions.

3 RESULTS

Using the FluxEs program arbitrary metabolic pathways can be modeled. For the *in vivo* validation experiment, a model of the TCA cycle was implemented (Fig. 1) and its flux parameters were optimized to fit the experimentally measured NMR multiplets. Oxygen consumption is stoichiometrically coupled to TCA cycle flux and could therefore be directly calculated from two of these parameters (Chatham *et al.*, 1995) [Equation (1)]. The optimization criterion used for the parameter estimation consists of (i) the χ^2 between the NMR multiplets computed by FluxEs and the NMR multiplets experimentally measured in the LIPSSS experiment and (ii) previous knowledge about model parameters added via Bayesian priors [Equation (2)]. The validation experiments were performed on 14 pig hearts *in vivo* under two different metabolic conditions: basal state and cardiac stress induced by dobutamine. In the same hearts, myocardial oxygen consumption was quantified from blood gas and blood flow measurements. This classic physiological 'gold standard' (Alders *et al.*, 2004) was compared with the LIPSSS oxygen consumption calculated from the parameter estimates [Equation (4)].

3.1 Simulations

In order to determine an appropriate parameter estimation strategy, we investigated a range of metabolic conditions of the data measured in the LIPSSS experiments. Hierarchical clustering revealed four clusters in each of the two experimental groups. To simulate the conditions represented by these eight clusters, we generated 25 synthetic noisy datasets for each of these clusters under controlled conditions, i.e. with known model parameters. The shape of the parameter space was analyzed and parameters were re-estimated from the synthetic data (Section 2).

The investigation of the parameter space revealed a 'golf course' landscape with shallow slopes and, sometimes multiple, narrow minima (see Fig. 2 and Supplementary Material). We found 'sloppy'

parameter combinations (Gutenkunst *et al.*, 2007), e.g. when J_{tca} and P_{dil} are both increasing the value of χ^2_{prior} does change little, indicated by the diagonally oriented valleys in the χ^2_{prior} landscape around the global optimum (Fig. 2A). Other parameter combinations showed low cross-sensitivity (e.g. J_{tca} and J_{exc}) indicated by horizontal or vertical χ^2_{prior} troughs around the global optimum (Fig. 2B). Since simulation showed the difficulty of the parameter estimation in shallow parameter landscapes using random start values, we designed another strategy based on a partial grid search to find better start values for parameter fitting.

During the initial parameter re-estimation all parameters (J_{tca}, J_{exc}, T_{trans} and P_{dil}) except P_{anap} were free between a minimum and maximum value. Based on literature information (Martini *et al.*, 2002; Panchal *et al.*, 2000, 2001), P_{anap} was coupled to a Bayesian prior with an expected value of $6\% \pm 3\%$ of the TCA cycle flux J_{tca}. Simulations showed that if prior knowledge on P_{anap} is not used, its values reach physiologically impossible regions and make the estimation of the remaining parameters less precise. The results of the parameter estimation are given in Figure 3 (one prior) and demonstrate that estimation of J_{tca}, T_{trans} and P_{dil} is possible within small standard errors and without prior knowledge. As expected, the estimation of P_{anap} was good due to the prior knowledge. However, parameter estimation with prior values for P_{anap} deliberately set wrong (Supplementary Material) show that the remaining parameters have a low sensitivity for this parameter. In contrast, the estimation of J_{exc} is much more difficult and often shows a high variety in the estimates. Nevertheless, just like P_{anap}, J_{exc} does not sensitively affect the remaining parameters.

In order to improve the estimation of the parameters J_{tca} and P_{dil} on datasets with few multiplets, we also constrained parameters J_{exc} and T_{trans} with additional Bayesian priors (Section 2). The parameter estimates are given in Figure 3 (three priors) and demonstrate that the standard deviation of J_{tca} and P_{dil} was decreased with 19% and 39% on average. There is no sensitive influence for the parameter estimates of J_{tca} and P_{dil} by the additionally prior constrained parameters (J_{exc} and T_{trans}), see Figure 3 (one prior and three priors). Next, this strategy derived from the simulations was applied to the experimental data below.

3.2 Testing flux estimation in cardiac tissue samples *in vivo*

We tested the new analysis methods for the LIPSSS data by quantitating aerobic metabolic fluxes *in vivo* in pig hearts. Acetate enriched with ^{13}C was infused in a coronary artery in anesthetized pigs (Section 2). ^{13}C NMR spectra of glutamate in extracts of multiple contiguous samples from each heart were measured. Up to nine multiplet intensities were obtained and analyzed with the FluxEs package to determine the five metabolic parameters of the TCA cycle model. Results for the five metabolic parameters for each heart are given in Figure 4. One heart of the dobutamine group was excluded because only one of its eight samples lead to acceptable parameter estimates (Section 2). The standard error of the mean reflects both real measurement error and true spatial variation of metabolism among the samples. Spatial variation is substantial in the heart at the level of TCA cycle enzyme activities and blood supply of oxygen: blood flow and succinate dehydrogenase enzyme activity have a true spatial SD of about 20–25% of their average

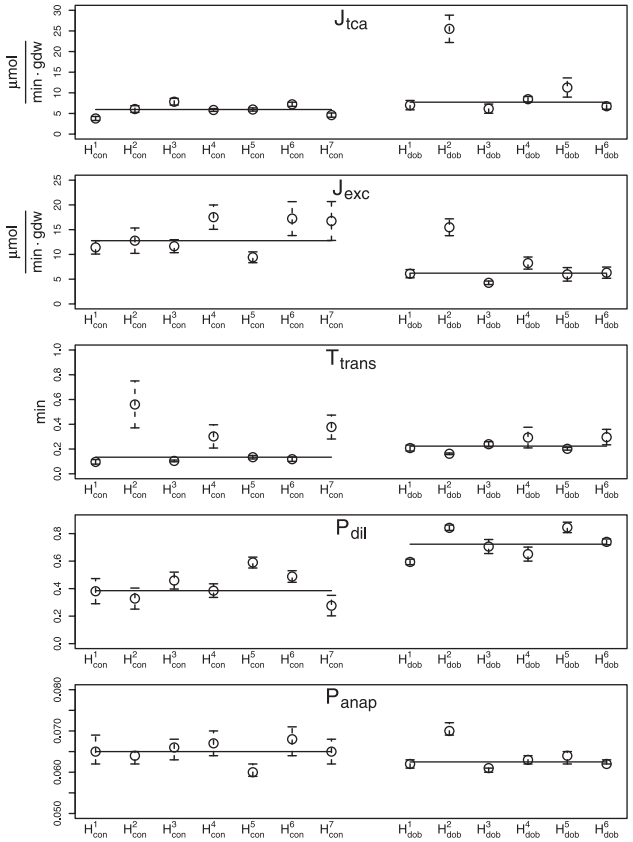

Fig. 4. Average parameter estimates (open circles) with standard error achieved on the seven hearts of the control group (left) and the six hearts of the dobutamine group (right). The horizontal lines show the median of the particular parameter estimate among all hearts of a group.

values across samples of about 40–200 mg dry mass (Alders *et al.*, 2004 and references cited there).

Despite this substantial contribution of spatial variation across the samples in each heart, the standard error of the mean for J_{tca} was of order 9.5% in the control and 14.3% in the dobutamine group. Based on the standard error of J_{tca} in the simulations, which was calculated using the known NMR measurement error (Fig. 3), we estimate that on average 1.3 μmol/min·gdw of the standard error of J_{tca} for the heart (Fig. 4) are due to real spatial variation. The remaining error is due to measurement error. The acetate uptake, determined by $J_{tca} \cdot (1 - P_{dil})$ (Fig. 1), is on average 3.53 ± 0.48 μmol/min·gdw in the control group and 2.53 ± 0.49 μmol/min·gdw with dobutamine. These measurements clearly show differences in energy metabolism across 13 of the 14 hearts. The increase of TCA cycle flux induced by dobutamine reflects the higher cardiac workload (O'Donnell *et al.*, 2004). In addition, parameter P_{dil} demonstrates increased dilution of acetate with other carbon substrates as found previously with *in vivo* NMR (Robitaille *et al.*, 1993). The estimates of J_{exc} show that it is lower during dobutamine stimulation. This is in excellent agreement with a report on reduced ^{13}C label transfer from α-ketoglutarate to cytosolic glutamate during myocardial dobutamine stress (O'Donnell *et al.*, 2004). Please note that the pig with heart H^2_{dob} (Fig. 4) showed by far the strongest response to dobutamine: its heart rate increased to 210 beats per minute

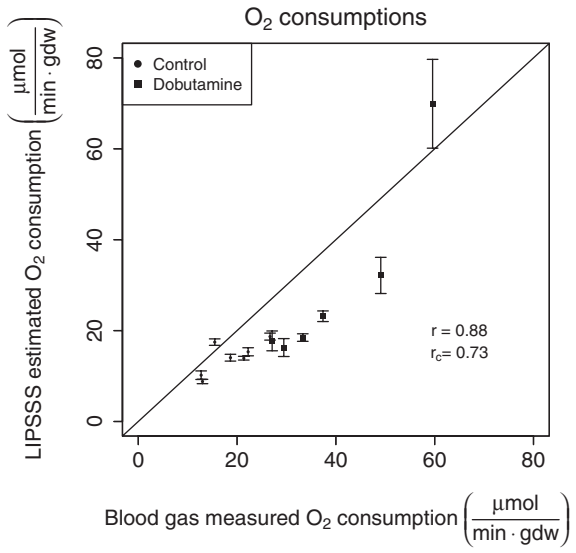

Fig. 5. Comparison of oxygen consumption estimated from LIPSSS model parameters and 'gold standard' oxygen consumptions, measured in pig hearts *in situ*. Data points are calculated according to Equation (4) and are close to the unity line. The error bars indicate the propagated error of the parameter estimates of J_{tca} and P_{dil} [Equation (3)], calculated from the individual tissue sample estimates. Pearson's correlation is given as r and Lin's concordance coefficient (indicating the agreement between a new set of observations and the original set) as r_c. The equation of the regression line is: $y = 0.78x + 11.57$.

compared with 130–178 beats per minute for the other hearts. This explains the high J_{tca} and J_{exc}.

3.3 Testing oxygen consumption

The quantification of J_{tca} and P_{dil} using NMR multiplet intensities from LIPSSS experiments means that the oxygen consumption in individual samples [Equation (1)] and hence for entire hearts [Equation (4)] can be calculated. We therefore compared the calculated oxygen consumption based on the LIPSSS method in the tissue samples with independently measured oxygen consumption determined from classic blood gas oxygen and blood flow measurements. The value calculated from LIPSSS agreed with the 'gold standard' physiological measurements (Fig. 5), despite the fact that the small tissue samples covered only part of the much larger area that was covered by the blood gas oxygen measurement. The overall correlation coefficient is $r = 0.88$ ($n = 13$, $P < 10^{-4}$) and control and dobutamine group are clearly separated. The LIPSSS method only measures oxygen consumption linked to TCA cycle flux. Additional oxygen consumption is also covered by the blood gas measurements (Challoner, 1968; van Beek *et al.*, 1999), which may explain part of the higher values. We conclude that there is agreement between the new method using LIPSSS analyzed with FluxEs and independent 'gold standard' measurements.

4 DISCUSSION

We developed and tested analysis methods and software for quantitation of metabolic fluxes by *in silico* simulation of the LIPSSS protocol and validated the approach *in vivo* in animal LIPSSS experiments. LIPSSS experiments entail that stable isotope-enriched metabolic substrates are given to the biological system and that the level of incorporation of the label in a brief, well-defined period of time allows determining the speed of metabolic turnover by computational analysis.

As revealed by simulation (Fig. 3), the parameter estimates for J_{tca} and P_{dil} show low standard errors and were not sensitive to values of the parameters J_{exc}, T_{trans} and P_{anap}. This means that the variations in J_{exc}, T_{trans} and P_{anap} have only small effects on the estimation of J_{tca} and P_{dil}. Therefore, we chose to restrict J_{exc}, T_{trans} and P_{anap} by prior knowledge encoded in Bayesian priors to improve the estimation of J_{tca} and P_{dil}. Furthermore, the *in vivo* experiments show that J_{tca}, J_{exc} and P_{dil} reveal the expected physiological differences between the control and the dobutamine-stressed hearts.

Individual differences between the pigs were expected and indeed observed (Figs 4 and 5). Oxygen consumption calculated from model parameters corresponds with oxygen consumption measured from blood gas and are close to the line of identity. It is expected that oxygen consumption determined from blood gas is higher than oxygen consumption calculated from the TCA cycle measured with the LIPSSS protocol. The blood gas uptake includes other oxygen consuming reactions, e.g. catalyzed by oxygenases or reactive oxygen species formation in addition to the oxygen consumption linked to the TCA cycle. Oxygen consumption calculated using LIPSSS data reflects only the reaction with reducing equivalents produced in the TCA cycle flux. This is in accordance with the findings of Challoner (1968). Hence, the expected oxygen consumption calculated using LIPSSS data is lower than uptake of oxygen from the blood. Measurements of other oxygen consuming reactions should be added to TCA cycle-based calculations if one wants to precisely predict oxygen uptake from the blood. The differences in metabolism between hearts of the control and dobutamine group are reflected by the higher average oxygen consumption in the dobutamine group (high workload) compared with the control group.

We have preliminary evidence that in future versions of the software package (FluxEs 2.0) it is possible to implement (i) on the fly C code generation that makes simulations 15 times faster, (ii) determination of optimal start values for parameter optimization using a particle swarm algorithm (Kennedy and Eberhart, 1995), (iii) simulation of NMR multiplet time series for multiple metabolites, (iv) parameter optimization using NMR multiplet time series of multiple metabolites, and (v) multiple nonlinear optimization routines.

In conclusion, FluxEs is a framework designed for parameter estimation in metabolic models by fitting simulated NMR multiplets against multiplets measured during LIPSSS experiments. FluxEs can flexibly handle arbitrary metabolic pathways that are not in isotopic steady state and will work on most computer operating systems. FluxEs was validated on NMR measurements from multiple tissue biopsies from pig hearts. The LIPSSS protocol, based on taking biopsies at a single time point, potentially has much higher spatial and biochemical resolution than *in vivo* NMR experiments. We anticipate that the LIPSSS approach in combination with the easy to use computer package FluxEs will prove applicable to many metabolic pathways and biological systems, such as central metabolism in cancer biopsies as well as neurotransmitter and central metabolism in neural cell cultures and animal studies.

Funding: This work is supported by a BSIK grant through the Netherlands Genomics Initiative (NGI). The work is part of the BioRange program (project number SP 2.2.1) of the Netherlands Bioinformatics Centre (NBIC) and also part of the Center for Medical Systems Biology which is a Genomics Center of Excellence funded by the Dutch Government via the NGI.

Conflict of Interest: none declared.

REFERENCES

Alders,D.J.C. *et al.* (2004) Myocardial oxygen consumption in porcine left ventricle is heterogeneously distributed in parallel to heterogeneous oxygen delivery. *Am. J. Physiol. Heart Circ. Physiol.*, **287**, H1353–H1361.

Antoniewicz,M.R. *et al.* (2007) Elementary metabolite units (EMU): a novel framework for modeling isotopic distributions. *Metab. Eng.*, **9**, 68–86.

Bassingthwaighte,J.B. and Beard,D.A. (1995) Fractal ^{15}O-labeled water washout from the heart. *Circ. Res.*, **77**, 1212–1221.

Binsl,T.W. *et al.* (2007) FluxSimulator: an R package to simulate isotopomer distributions in metabolic networks. *J. Stat. Softw.*, **18**, 1–18.

Brown,K.S. and Sethna,J.P. (2003) Statistical mechanical approaches to models with many poorly known parameters. *Phys. Rev. E.*, **68**, 1–9.

Carvalho,R.A. *et al.* (2001) TCA cycle kinetics in the rat heart by analysis of ^{13}C isotopomers using indirect ^{1}H[^{13}C] detection. *Am. J. Physiol. Heart Circ. Physiol.*, **281**, H1413–H1421.

Challoner,D.E. (1968) Respiration in myocardium. *Nature*, **217**, 78–79.

Chance,E.M. *et al.* (1983) Mathematical analysis of isotope labeling in the citric acid cycle with applications to ^{13}C NMR studies in perfused rat hearts. *J. Biol. Chem.*, **258**, 13785–13794.

Chatham,J.C. *et al.* (1995) Calculation of absolute metabolic flux and the elucidation of pathways of glutamate labeling in perfused rat hearts by ^{13}C NMR spectroscopy and nonlinear least squares analysis. *J. Biol. Chem.*, **270**, 7999–8008.

Gutenkunst,R.N. *et al.* (2007) Universally sloppy parameter sensitivities in systems biology models. *PLoS Comput. Biol.*, **3**, 1–10.

Hindmarsh,A. (1983) ODEPACK, a systematized collection of ODE solvers. *Sci. Comput.*, **1**, 55–64.

Kelleher,J.K. (2001) Flux estimation using isotopic tracers: common ground for metabolic physiology and metabolic engineering. *Metab. Eng.*, **3**, 100–110.

Kennedy,J. and Eberhart,R.C. (1995) Particle swarm optimization. In *Proceedings of the 6th International Symposium on Micro Machine and Human Science*, IEEE press, Piscataway, NJ, USA, pp. 39–43.

Malloy,C.R. *et al.* (1990) Analysis of tricarboxylic acid cycle of the heart using ^{13}C isotope isomers. *Am. J. Physiol. Heart Circ. Physiol.*, **259**, H987–H995.

Martini,W.Z. *et al.* (2002) Quantitative assessment of anaplerosis from propionate in pig heart *in vivo*. *Am. J. Physiol. Endoc. Metab.*, **284**, 351–356.

Nöh,K. and Wiechert,W. (2006) Experimental design principles for isotopically instationary ^{13}C labeling experiments. *Biotechnol. Bioeng.*, **10**, 233–251.

O'Donnell,J.M. *et al.* (2004) Limited transfer of cytosolic NADH into mitochondria at high cardiac workload. *Am. J. Physiol. Heart Circ. Physiol.*, **286**, H2237–H2242.

Panchal,A.R *et al.* (2000) Partitioning of pyruvate between oxidation and anaplerosis in swine hearts. *Am. J. Physiol. Heart Circ. Physiol.*, **279**, 2390–2398.

Panchal,A.R. *et al.* (2001) Acute hibernation decreases myocardial pyruvate carboxylation and citrate release. *Am. J. Physiol. Heart Circ. Physiol.*, **281**, 1613–1620.

Pound,K.M. *et al.* (2009) Substrate—enzyme competition attenuates upregulated anaplerotic flux through malic enzyme in hypertrophied rat heart and restores triacylglyceride content - attenuating upregulated anaplerosis in hypertrophy. *Circ. Res.*, **104**, 805–812.

Prinzen,F.W and Bassingthwaighte,J.B. (2000) Blood flow distributions by microsphere deposition methods. *Cardiovasc. Res.*, **45**, 13–21.

Quek,L. *et al.* (2009) OpenFLUX: efficient modelling software for ^{13}C-based metabolic flux analysis. *Microb. Cell. Fact.*, **8**, 1–15.

Randle,P.J. *et al.* (1970) Control of the tricarboxylate cycle and its interactions with glycolysis during acetate utilization in rat heart. *Biochem. J.*, **117**, 677–695.

Robitaille,P.L. *et al.* (1993) Dynamic ^{13}C NMR analysis of oxidative metabolism in the *in vivo* canine myocardium. *J. Biol. Chem.*, **268**, 26296–26301.

Sherry,A.D. *et al.* (1998) Effects of aminooxyacetate on glutamate compartmentation and TCA cycle kinetics in rat hearts. *Am. J. Physiol. Heart Circ. Physiol.*, **274**, 591–599.

Sherry,A.D. *et al.* (2004) Analytical solutions for ^{13}C isotopomer analysis of complex metabolic conditions: substrate oxidation, multiple pyruvate cycles, and gluconeogenis. *Metab. Eng.*, **6**, 12–24.

van Beek,J.H.G.M. *et al.* (1998) Simple model analysis of ^{13}C NMR spectra to measure oxygen consumption using frozen tissue samples. *Adv. Exp. Med. Biol.*, **454**, 475–485.

van Beek,J.H.G.M. *et al.* (1999) A ^{13}C NMR double-labeling method to quantitate local myocardial O_2 consumption using frozen tissue samples. *Am. J. Physiol. Heart Circ. Physiol.*, **277**, H1630–H1640.

Vanhamme,L. *et al.* (1997) Improved method for accurate and efficient quantification of MRS data with use of prior knowledge. *J. Magn. Reson.*, **129**, 35–43.

Wiechert,W. (2001) ^{13}C metabolic flux analysis. *Metab. Eng.*, **3**, 195–206.